Generation of hierarchical pore systems in the titanosilicate ETS-10 by hydrogen peroxide treatment under microwave irradiation†

Claudiu C. Pavel and Wolfgang Schmidt*

Received (in Cambridge, UK) 11th November 2005, Accepted 15th December 2005
First published as an Advance Article on the web 19th January 2006
DOI: 10.1039/b515720j

Supermicropores and well-defined mesopores with an average size of 10 nm were created in ETS-10 structure by post-synthesis treatment with H_2O_2 under microwave irradiation. Macropores were also formed and the external surface area of the material was increased during the treatment.

Zeolites are aluminosilicates with crystal structures forming channels and cavities in the nanometer range. These micropores show regular spatial arrangements and the pore dimensions are characteristic for each particular structure type.[1] The specific properties of zeolites make them excellent catalysts, *e.g.* for petrochemical processes. Besides their highly favorable role in providing shape selectivity, the presence of micropores may sometimes limit the catalytic performance of zeolites.[2] The reason for this is intra-crystalline diffusion limitation, as a result of the slow gas transport of reactants and products in the channels of larger catalyst particles.[3] Solutions to minimize diffusion limitation in zeolites are the reduction of the intra-crystalline diffusion pathlength by using extremely small zeolite crystals[4] or the generation of larger transport pores with improved diffusional properties. In some studies, zeolites were assembled into an ordered mesoporous structure by deposition of small zeolite crystals on the pore walls of mesoporous materials[5] or by re-crystallization of the amorphous pore walls of mesoporous silicates into zeolite materials.[6,7] However, a more generally applied strategy to attain materials combining zeolite micropores with larger mesopores is the intra-crystalline generation of mesopores in the zeolite structure. Different approaches for the generation and characterization of mesopores in zeolite crystals and their impact on the catalytic activity have been recently reported in a review article.[8] Conventional steaming at relatively high temperature, leaching in acidic or alkaline media, chemical treatments (reaction with $SiCl_4$, EDTA or $(NH_4)_2SiF_6$), as well as creation of mesopores during synthesis, such as using carbon templates, have been applied to obtain hierarchically structured porous materials containing both micro- and mesoporosity.

This communication describes a novel simple approach to generate extra-porosity into the titanosilicate ETS-10 possessing a three-dimensional system of interconnected micropores with dimensions of about 0.8 × 0.5 nm.[9,10] The ETS-10 structure has a number of characteristics making it particularly interesting as prospective catalyst in heterogeneous catalysis.[11] The activity of ETS-10 can be enhanced by post-synthesis modifications and then be used, for instance, as shape-selective photocatalyst in the degradation of aromatic molecules.[12]

We investigated the effect of hydrogen peroxide treatment combined with microwave (MW) irradiation as a method to form larger pores into the titanosilicate structure, aiming for larger micro- and mesopores but still preserving the basic structural characteristics of the parent material.

The synthesis of ETS-10 was performed using a gel with the composition: 5.0 SiO_2 : 1.0 TiO_2 : 7.0 Na_2O : 0.75 K_2O : 150 H_2O. The gel was autoclaved under autogenous pressure for 7 days at 190 °C. The obtained solid product was filtered and washed with de-ionized water and dried overnight at 90 °C. The XRD pattern of the crystalline sample proved it to be pure ETS-10.[9] The post-synthesis treatment was performed as follows: 200 mg of dried powder was mixed with 20 mL H_2O_2 (10–30 wt%) solution and loaded in a MARS-5 microwave oven (CEM) equipped with teflon autoclaves. This mixture was heated with 600 W microwave power to 150 °C and kept at this temperature for 15 min. The solid was recovered by filtration, washed and dried overnight at 80 °C. All H_2O_2-treated samples showed excellent crystallinity as investigated by XRD measurements (see ESI†).

The changes of the pore characteristics of the solids upon post-synthesis treatment were studied by physical gas adsorption and by transmission electron microscopy. Nitrogen and argon adsorption/desorption isotherms at 77 K and 87 K, respectively, were recorded on a Micromeritics ASAP 2010 instrument. Prior to the measurements, the samples were activated by heating them to 300 °C under vacuum overnight. Argon adsorption at 87 K was used for accurate determination of micropore size distributions. The pore size distributions calculated by non-local density functional theory (NLDFT) of the parent ETS-10 and MW-H_2O_2/ETS-10 are shown in Fig. 1.

Transmission electron micrographs were obtained on a Hitachi 7500 transmission electron microscope operating with an acceleration voltage of 100 kV.

Determination of exact pore dimensions cannot be expected since the micropores of ETS-10 have an elliptic shape (0.5 × 0.8 nm). The pore sizes calculated from sorption data thus typically result in an average pore diameter; here about 0.72 nm for as-made ETS-10. For H_2O_2-treated samples, a bimodal micropore size distribution is observed (Fig. 1). The second type of pores corresponds to larger micropores (supermicropores). They are probably created upon extraction of Ti atoms together with next-neighbor SiO_4 tetrahedra (= ($Ti^{[6]}$,$Si^{[4]}$)-spiro-5 units) from

Max-Planck-Institut für Kohlenforschung, Kaiser Wilhelm Platz 1, D-45470, Mülheim an der Ruhr, Germany.
E-mail: wolfgang.schmidt@mpi-muelheim.mpg.de; pavel@mpi-muelheim.mpg.de; Fax: +49 (0)208 3062995; Tel: +49 (0)208 3062370

† Electronic supplementary information (ESI) available: XRD patterns and nitrogen adsorption/desorption isotherms of the samples. See DOI: 10.1039/b515720j

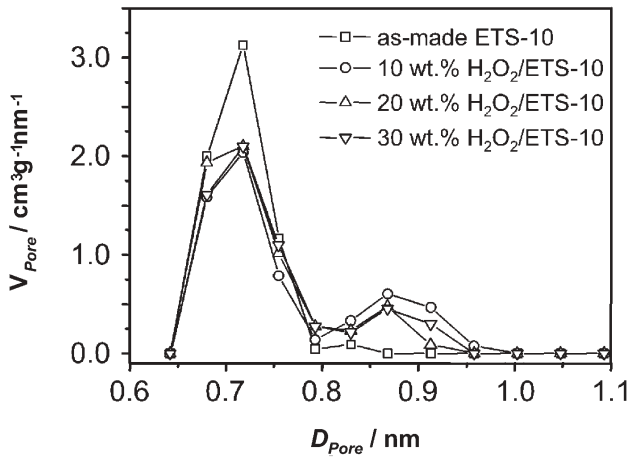

Fig. 1 Micropore size distribution of different ETS-10 samples as calculated from the argon adsorption branch by NLDFT method.

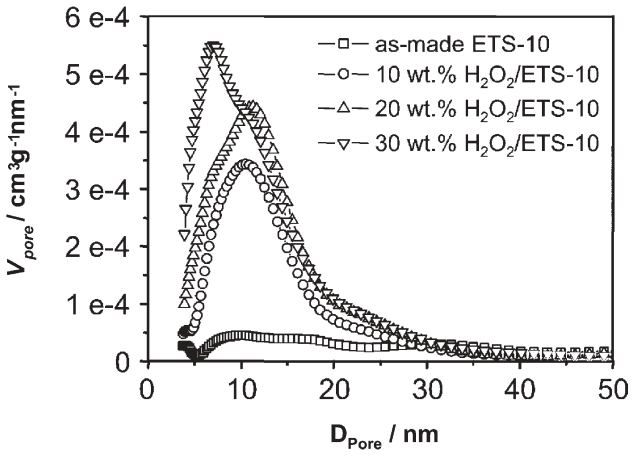

Fig. 3 Mesopores size distribution of as-made ETS-10 and MW/H_2O_2-ETS-10 samples as calculated by NLDFT method.

the structure upon H_2O_2 treatment (inset Fig. 4). Double pore defects due to stacking faults are known to be present in as-made ETS-10.[10] However, the supermicropores formed during the H_2O_2 treatment presumably correspond to a larger pore with theoretical dimension of 0.76 × 1.98 nm calculated from crystallographic data using the structure data reported by Wang and Jacobson[13] (Fig. 2). The sorption data again only give an average size and do not reflect the real dimensions of the highly elliptic pores.

It is important to note that the formation of such supermicropores was also observed after contact of ETS-10 with hydrogen peroxide at room temperature without application of microwave irradiation.[14]

After microwave assisted H_2O_2 treatment, ETS-10 samples showed an enhanced uptake of N_2 at higher relative pressures accompanied by a hysteresis loop (see ESI†), indicating the presence of a mesopore system in these samples. The NLDFT pore size distribution derived from the N_2 adsorption branch of the isotherms shows the presence of mesopores with sizes of about 10 nm (Fig. 3).

The generation of large mesopores after post-synthesis treatment in the size range of 5–20 nm is evident. The mesopore volume is slightly increased with increasing H_2O_2 concentration. The average size and distribution of mesopores can be controlled by varying H_2O_2 concentration, contact time and temperature. Systematic investigations showed that mesoporosity starts to develop at 100 °C even at low H_2O_2 concentration. At 150 °C a quite narrow distribution of mesopores centered at about 7 and 10 nm is observed depending of the H_2O_2 concentration used (see Fig. 3). Transmission electron microscopy (TEM) allowed visualization of the pore systems of modified ETS-10 as shown Fig. 4.

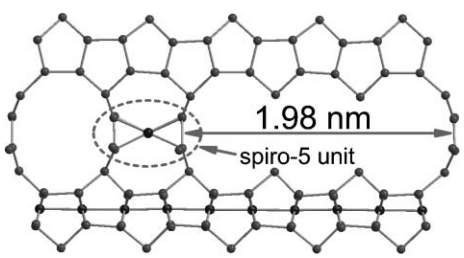

Fig. 2 Structural representation of the supermicropores in ETS-10 which would form after leaching of spiro-5 units. Oxygen atoms connecting neighbouring atoms Si and Ti were omitted for simplicity.

A TEM image is a projection of the mass-density encountered by electrons passing through the sample and pores show up as bright areas. The inset shows the extended supermicropores and the main image clearly shows the mesopores. Both supermicropores and mesopores seem to be aligned parallel to Ti–O–Ti chains in the ETS-10 structure. These Ti–O–Ti chains are oriented perpendicular to each other in two dimensions and their removal results in pores oriented mainly along these chains. Fig. 4 clearly shows the parallel alignment of the mesopores. The bright circular areas represent views into mesopores oriented exactly perpendicular to the straight ones in the image plane (Fig. 4). The mesopores size estimated from TEM images is in good agreement with the pore size distribution derived from NLDFT (N_2 adsorption) centered around 10 nm.

It is known that microwave irradiation is more efficient for transferring thermal energy to a given volume of material than conventional thermal processing. Therefore, H_2O_2/ETS-10 treatment under microwave irradiation and uniform batch stirring leads in a short time to removal of a significant part of the Ti and

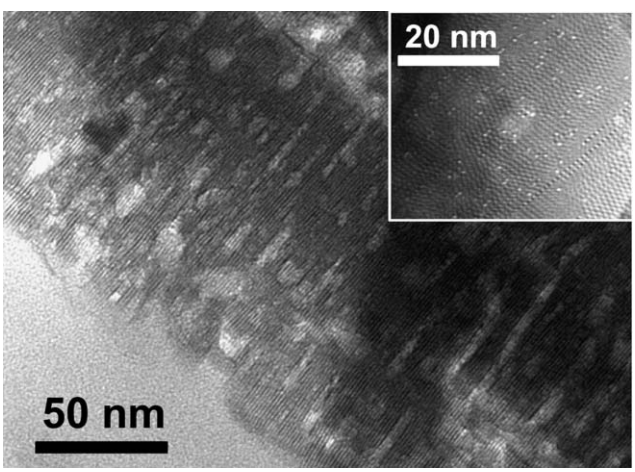

Fig. 4 TEM micrograph of MW/20 wt% H_2O_2-treated ETS-10 sample. High resolution image in insert visualizes the supermicropores.

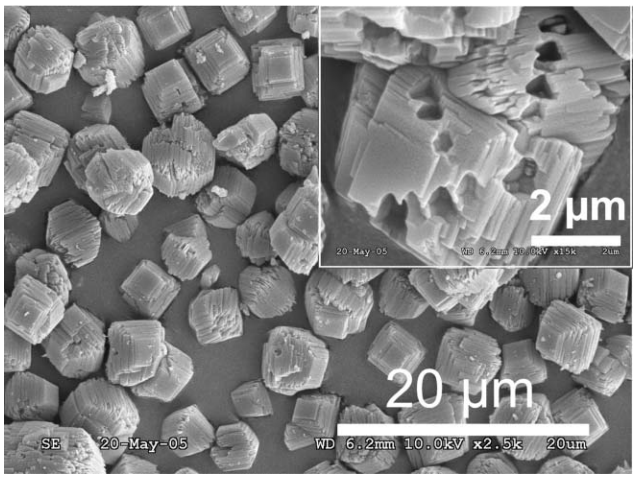

Fig. 5 SEM images of MW/30 wt% H_2O_2-treated ETS-10 crystals.

Si from the structure. This results in the formation of larger pores, such as supermicro- and mesopores, but still preserving the microporosity and structural integrity of the material.

The presence of mesopores in the ETS-10 structure will change the external surface area of material. The external surface area of the crystallites, as calculated by the *t*-plot method on top of the microporous plateau, increases with increasing concentration of hydrogen peroxide as follows: 7 $m^2\ g^{-1}$ for as-made ETS-10, 19 $m^2\ g^{-1}$ for 10 wt% H_2O_2, 29 $m^2\ g^{-1}$ for 20 wt% H_2O_2, and 42 $m^2\ g^{-1}$ for 30 wt% H_2O_2. However, the external surface area calculated in this way corresponds to the total surface area of meso- and macropores. If the crystallite size and morphology would remain unchanged, the difference between the external surface area of the treated ETS-10 and as-made ETS-10 would be the surface area of the mesopores created. Scanning electron microscopy images measured on a Hitachi S-3500 N microscope showed that the crystal surfaces of ETS-10 did not remain unaltered during the H_2O_2 treatment (Fig. 5).

The ETS-10 crystals have a typical bipyramidal truncated morphology with a pseudo-4-fold symmetry along *c* axis in accord with those described by Rocha and Anderson.[11] Traces of faults perpendicular to this axis formed during crystallization process are also clear visible. H_2O_2 treatment combined with microwave irradiation leads to the formation of macropore-like defects on the surface of crystals (inset Fig. 5). Applying the *t*-plot on top of the mesopore plateau (Harkins/Jura thickness range of 15–18 Å) allowed distinction between the surface area induced by meso- and macropores, respectively. Formation of extended surface defects lead to augmentation of external surface area due to macropores with macropore surface areas of: 12 $m^2\ g^{-1}$ for 10 wt% H_2O_2, 12 $m^2\ g^{-1}$ for 20 wt% H_2O_2, and 18 $m^2\ g^{-1}$ for 30 wt% H_2O_2.

It has been recently shown that the catalytic centers for photodegradation of phenols on ETS-10 of different crystal sizes are mainly located on the surface of the crystals, whereas the internal pore system of ETS-10 rather protects molecules against degradation.[15] An increase of external surface area, as a contribution of both meso- and macropores, similar to that of TiO_2 (*ca.* 50 $m^2\ g^{-1}$), could thus lead to an enhancement of active catalytic sites. In this way, the photocatalytic activity of modified-ETS-10 may become comparable or even better to that of the rather unselective TiO_2.

In summary, we have shown that the hydrogen peroxide combined with microwave irradiation treatment results in hierarchical pore systems in the titanosilicate ETS-10 due to generation of intra-crystalline supermicropores and mesopores with well preserved microporosity and structural integrity. The mesopore size and volume is depending on the H_2O_2 concentration, treatment time and temperature and under specific conditions, mesopores with a narrow size distribution centered around 10 nm can be obtained. Furthermore, this treatment induces defects on the crystals surface contributing to an increased external surface area and macroporosity of the materials. The generation of larger pores into the ETS-10 structure makes these materials very promising candidates for various catalytic applications because diffusion limitations should be significantly reduced due to the formation of the hierarchical pore system providing both shape-selective micropores and larger transport pores. In comparison to the mesopore systems of steamed or acid/base-leached zeolites, the mesopores of the ETS-10 materials obtained by microwave-assisted H_2O_2 treatment are very uniform and seem to be even oriented inside the crystallites. We are currently investigating the diffusion characteristics of the materials in catalytic applications and the result of these investigations will be reported in due course.

We would like to thank A. Dreier, B. Tesche, and H. Bongard for TEM and SEM measurements and financial support by the DFG (Schm 936/4-1) and Max Planck Society is gratefully acknowledged.

Notes and references

1 W. M. Meier and D. H. Olson, in *Atlas of Zeolite Structure Types*, Butterworth-Heinemann, London, 1992.
2 J. Kärger and D. M. Ruthven, in *Diffusion in Zeolite and Other Microporous Materials*, John Wiley and Sons, New York, 1992.
3 X. Zhao, G. Q. Lu and G. J. Millar, *Ind. Eng. Chem. Res.*, 1996, **35**, 2075; A. Corma, A. Martinez and V. Martinez-Soria, *J. Catal.*, 2001, **200**, 259; M. Ogura, S. Y. Shinomiya, J. Tateno, Y. Nara, M. Nomura, E. Kikuchi and M. Matsukata, *Appl. Catal., A*, 2001, **219**, 33; J. Pérez-Ramírez, F. Kapteijn, J. C. Groen, A. Doménech, G. Mul and J. A. Moulijn, *J. Catal.*, 2003, **214**, 33.
4 E. A. Swabb and B. C. Gates, *Ind. Eng. Chem. Fundam.*, 1972, **11**, 540; W. O. Haag, R. M. Lago and P. B. Weisz, *Faraday Discuss. Chem. Soc.*, 1982, **72**, 317; K. Rajagopalan, A. W. Peters and G. C. Edwards, *Appl. Catal.*, 1986, **23**, 69; P. Voogd and H. van Bekkum, *Appl. Catal.*, 1990, **59**, 311; G. Bellussi, G. Pazzuconi, C. Perego, G. Girotti and G. Terzoni, *J. Catal.*, 1995, **157**, 227.
5 A. Karlsson, M. Stöcker and R. Schmidt, *Microporous Mesoporous Mater.*, 1999, **27**, 181.
6 K. R. Kloestra, H. van Bekkum and J. C. Jansen, *Chem. Commun.*, 1997, **23**, 2281.
7 L. Huang, W. Quo, P. Deng, Z. Xue and Q. Li, *J. Phys. Chem. B*, 2000, **104**, 2817.
8 S. van Donk, A. H. Janssen, J. H. Bitter and K. P. de Jong, *Catal. Rev. Sci. Eng.*, 2003, **45**, 297.
9 M. W. Anderson, O. Terasaki, T. Ohsuna, A. Philippou, S. P. MacKay, A. Ferreira, J. Rocha and S. Lidin, *Nature*, 1994, **367**, 347.
10 M. W. Anderson, O. Terasaki, T. Ohsuna, P. J. O. Malley, A. Philippou, S. P. MacKay, A. Ferreira, J. Rocha and S. Lidin, *Philos. Mag. B*, 1995, **71**, 813.
11 J. Rocha and M. W. Anderson, *Eur. J. Inorg. Chem.*, 2000, 801.
12 F. X. Llabrés i Xamena, P. Calza, C. Lamberti, C. Prestipino, A. Damin, S. Bordiga, E. Pelizzetti and A. Zecchina, *J. Am. Chem. Soc.*, 2003, **125**, 2264.
13 X. Wang and A. J. Jacobson, *Chem. Commun.*, 1999, 973.
14 C. C. Pavel, S.-H. Park, A. Dreier, B. Tesche and W. Schmidt, *Chem. Mater.*, 2006, submitted for publication.
15 P. Calza, C. Pazé, E. Pelizzetti and A. Zecchina, *Chem. Commun.*, 2001, 2130.

